Matter and Radiation at Extremes | RESEARCH ARTICLE | scitation.org/journal/mre

Projectile and target excitation in He^+ + He collisions at intermediate energies

Cite as: Matter Radiat. Extremes 6, 014404 (2021); doi: 10.1063/5.0025623
Submitted: 31 August 2020 • Accepted: 9 November 2020 •
Published Online: 15 December 2020

Junwen Gao,[1] Zhimin Hu,[1] Yong Wu,[2,3,a)] Jianguo Wang,[2] Nicolas Sisourat,[4] and Alain Dubois[4]

AFFILIATIONS

[1]Laser Fusion Research Center, China Academy of Engineering Physics, 621900 Mianyang, China
[2]Institute of Applied Physics and Computational Mathematics, 100088 Beijing, China
[3]Center for Applied Physics and Technology, HEDPS, and School of Physics, Peking University, 100871 Beijing, China
[4]Sorbonne Université, CNRS, Laboratoire de Chimie Physique-Matière et Rayonnement, F-75005 Paris, France

Note: This paper is part of the Special Issue on Atomic and Molecular Physics for Controlled Fusion and Astrophysics.
[a)]**Author to whom correspondence should be addressed:** wu_yong@iapcm.ac.cn

ABSTRACT

We present *ab initio* calculations of cross sections for projectile and target excitation occurring in the course of He^+ + He collisions using a three-active-electron semiclassical nonperturbative approach. Intermediate impact energies ranging from 1 keV to 225 keV/u are considered. The results of our calculations agree well with available measurements for both projectile and target excitation in the respective overlapping energy regions. A comparison of our results with those of other theoretical calculations further demonstrates the importance of a nonperturbative approach that includes a sufficient number of channels. Furthermore, it is found that the cross sections for target excitation into singlet states show a valley centered at about 25 keV/u, resulting from competition with electron transfer to singlet projectile states. By contrast, the cross sections for target excitation into triplet states do not exhibit any such structures.

I. INTRODUCTION

He^+ + He is one of the simplest atomic collisional systems containing only three electrons. It is, however, sufficiently complex to give rise to the main types of inelastic reactions (electron capture, excitation, ionization, and their bielectronic counterparts) observed in ion–atom collisions, since both target and projectile carry active electrons. It has therefore attracted a great deal of interest for several decades.[1–22] The majority of these studies have concentrated on electron capture (charge transfer) processes, since these are generally the dominant channels at intermediate impact energies. By contrast, electronic excitations have not usually been included in these studies owing to the fact that they are comparatively less likely to be active at intermediate impact energies. For target excitations occurring in the course of He^+ and He collisions

$$He^+(1s) + He(1s^2) \rightarrow He^+(1s) + He(1snl\,^{1,3}L), \quad (1)$$

some experimental results can be found in Refs. 9, 12, 16, and 19 for impact energies ranging from 5 keV/u to 75 keV/u and for $nl = 2s, 2p$, and $3s$, while for the projectile excitation

$$He^+(1s) + He(1s^2) \rightarrow He^+(2l) + He(1s^2\,^1S), \quad (2)$$

only a single series of experimental data, in the energy range 6.25 keV/u–35 keV/u, has been published.[16]

From a theoretical point of view, the investigation of He^+ + He collisions in the intermediate impact energy region still remains a challenge: perturbative approaches or approximate calculations using a model potential with only one (or two) active electrons may be inadequate owing to electronic correlation effects and the strong coupling between various channels; see, e.g., Ref. 4. Early in 1967, the calculated cross sections for capture and target excitation into $He^*(1s2s^{1,3}S)$ were first reported by Sural *et al.*[20] using a three-electron coupled-channel method. These authors considered only six channels and neglected all of the momentum transfer phases. This model allowed the description of single-target excitation and transfer into the first excited states at low impact energies of 0.15 keV/u–10 keV/u. Note that direct projectile excitation was excluded. Later, both projectile and target excitation processes in He^+ + He collisions were investigated by Hildenbrand *et al.*[7] using an extended three-electron coupled-channel calculation for impact

energies of 2.5 keV/u–150 keV/u. Although they included more channels (up to 128) in their calculations, the couplings between S and P states were not taken into account. To the best of our knowledge, no other theoretical results for the processes in Eqs. (1) and (2) are available. However, large discrepancies still exist between the available experimental and calculated results. This is particularly unfortunate from the viewpoint of applications, since there is a growing awareness that accurate excitation cross sections are important elements in databases for modeling of astrophysical[23–25] and laboratory plasmas.[26–28]

In the present work, we investigate both projectile and target excitation processes presented in Eqs. (1) and (2) using a three-electron semiclassical asymptotic-state close-coupling (3eASCC) method. Focusing on the energy domain 1 keV/u–225 keV/u, we compare our cross sections with the experimental data and discuss the possible reasons for the disagreement with previous calculations. Furthermore, we find that the cross sections for target excitation to singlet states and projectile excitation show clear oscillations as a function of impact energy, which we further discuss and interpret.

The remainder of the paper is organized as follows. In Sec. II, we briefly outline the 3eASCC method used in the present calculations. Section III is devoted to a detailed analysis of state-selective projectile and target excitation cross sections and direct comparisons with available experimental and theoretical results. This is followed by our conclusions in Sec. IV. Atomic units are used throughout, unless explicitly indicated otherwise.

II. THEORY

In the present work, a three-electron semiclassical asymptotic-state close-coupling approach is employed to calculate the cross section of the electronic processes in Eqs. (1) and (2) occurring during He^+ + He collisions. Only the main features of the method are outlined here, and more details can be found in our previous works.[4,29–31]

The n_e-electron time-dependent Schrödinger equation (TDSE) is written as

$$\left(H_e - i\frac{\partial}{\partial t}\Big|_{\vec{r}_1,\vec{r}_2,\ldots,\vec{r}_{n_e}}\right)\Psi\left(\vec{r}_1,\vec{r}_2,\ldots,\vec{r}_{n_e},R(t)\right) = 0, \tag{3}$$

where

$$H_e = \sum_{i=1}^{n_e}\left[-\frac{1}{2}\nabla_i^2 + V_T(r_i) + V_P(r_i^p)\right] + \sum_{i<j}\frac{1}{|\vec{r}_i - \vec{r}_j|} \tag{4}$$

is the electronic Hamiltonian, and $\vec{r}_i$ and $\vec{r}_i^{\,p} = \vec{r}_i - \vec{R}(t)$ are the position vectors of the electrons with respect to the target and the projectile, respectively. The relative projectile–target position $\vec{R}(t)$ defines the trajectory, with $\vec{R}(t) = \vec{b} + \vec{v}t$ in the usual straight-line, constant-velocity approximation ($\vec{b}$ and $\vec{v}$ are the impact parameter and velocity; see Fig. 1 in Ref. 4). V_T and V_P are the electron–target and electron–projectile nuclear potentials, respectively.

The Schrödinger equation is solved by expanding the wavefunction on a basis set composed of spin-adapted states of the isolated collision partners,

$$\begin{aligned}\Psi\left(\vec{r}_1,\vec{r}_2,\ldots,\vec{r}_{n_e},\vec{R}(t)\right) = \sum_{n_T,n_P}\sum_{J=1}^{N_{(n_T,n_P)}}\Big[&a_J^{(n_T,n_P)}(t)\Phi_J^{(n_T,n_P)} \\ &\times\left(\vec{r}_1,\vec{r}_2,\ldots,\vec{r}_{n_e},\vec{R}(t)\right) \\ &\times\exp\left(-iE_J^{(n_T,n_P)}t\right)\Big],\end{aligned} \tag{5}$$

with

$$\begin{aligned}\Phi_{J\equiv(j_T,j_P)}^{(n_T,n_P)}&\left(\vec{r}_1,\vec{r}_2,\ldots,\vec{r}_{n_e},\vec{R}(t)\right) \\ &= \hat{\mathbb{P}}\Big[\phi_{j_T}^{T_{n_T}}\left(\vec{r}_1,\vec{r}_2,\ldots,\vec{r}_{n_T}\right)\phi_{j_P}^{P_{n_P}} \\ &\quad\times\left(\vec{r}_{n_T+1}^{\,p},\vec{r}_{n_T+2}^{\,p},\ldots,\vec{r}_{n_T+n_P}^{\,p}\right)\Big],\end{aligned} \tag{6}$$

where $N_{(n_T,n_P)}$ denotes the number of states (and corresponding energies) for which n_T and n_P ($n_T + n_P = n_e$) electrons are on the target and projectile, respectively. The multielectron states $\Phi^{(n_T,n_P)}$ are expressed as linear combinations of spin-adapted products of Gaussian-type orbitals (GTOs) centered on isolated collision partners. The operator $\hat{\mathbb{P}}$ in Eq. (6) ensures the permutation of any two electrons among n_e and the full antisymmetry of the total wavefunctions as well as of the asymptotic target and projectile states. Note that for all electrons, the projectile states $\phi_{j_P}^{P_{n_P}}$ contain plane-wave electron translation factors (ETFs), $\exp\left(i\vec{v}\cdot\vec{r} - i\frac{1}{2}v^2t\right)$, ensuring Galilean invariance of the results. Inserting Eqs. (5) and (6) into Eq. (3), we obtain a set of first-order coupled differential equations that can be written in matrix form as

$$i\frac{d}{dt}\mathbf{a}(t) = \mathbf{S}^{-1}\left(\vec{b},\vec{v},t\right)\mathbf{M}\left(\vec{b},\vec{v},t\right)\mathbf{a}(t), \tag{7}$$

where $\mathbf{a}(t)$ is the column vector of time-dependent expansion coefficients, and $\mathbf{S}$ and $\mathbf{M}$ are the overlap and coupling matrices, respectively. These equations are solved for a set of initial conditions (initial state i, b, and v) using a robust predictor–corrector time-step variable method developed by Shampine and Gordon.[32] Using the orthogonality properties of the asymptotic states, the probability of a transition $i \to f$ is given by the coefficients a_f ($\equiv a_J^{(n_T,n_P)}$) as

$$P_{fi}(b,v) = \lim_{t\to\infty}|\langle\Phi_f|\Psi\rangle|^2 = \lim_{t\to\infty}|a_f(t)|^2. \tag{8}$$

The corresponding integral (total) cross sections for the considered transition are calculated as

$$\sigma_{fi}(v) = 2\pi\int_0^{+\infty} bP_{fi}(b,v)\,db. \tag{9}$$

In the present calculations, a set of 19 GTO basis sets[4] (10 for l = 0 and 3 × 3 for l = 1) are used on both projectile and target centers, and a total of 1260 states (states of two electrons on target and one electron on projectile, and vice versa) are included in the calculations. These states can describe elastic, excitation, single electron capture, and double electron capture channels, as well as ionization through the inclusion of pseudostates with energy lying above ionization thresholds. The energies of the relevant bound states of He^+ and He included in the calculations are shown in Table I, in which good agreement (within 1%) with available data can be seen. Convergence tests on the cross sections are performed by comparing the present results with those from a smaller basis set (12 GTOs on each center, i.e., 6 for l = 0 and 2 × 3 for l = 1), which allows the inclusion of 582 states in total. The convergence is evaluated to be better than 1% for the total single electron transfer, about 10% for the state-resolved electron transfer cross sections, and about 20% for the cross sections of projectile and target excitation.

TABLE I. Comparison of energies (in a.u.) of He^+ and He obtained using the GTO basis set with the data from NIST.[33]

	He^+		He		
State	E_{GTO}	E_{ref}	State	E_{GTO}	E_{ref}
1*s*	−2.000	−2.000	$1s^2\ ^1S$	−2.893	−2.903
2*s*	−0.500	−0.500	$1s2s\ ^1S$	−2.145	−2.146
2*p*	−0.495	−0.500	$1s2s\ ^3S$	−2.175	−2.175
3*s*	−0.222	−0.222	$1s2p\ ^1P$	−2.121	−2.124
			$1s2p\ ^3P$	−2.130	−2.133
			$1s3s\ ^1S$	−2.058	−2.061
			$1s3s\ ^3S$	−2.068	−2.068

III. RESULTS AND DISCUSSION

We first investigate the excitation of the He target atom; see Eq. (1). Figures 1(a)–1(c) show the cross sections for target excitation (TE) to singlet $He(1s2s^1S, 1s2p^1P$, and $1s3s^1S)$ excited states, respectively. Previous experimental[9,12,16,19] and theoretical[7,20] results are also displayed for comparison. Our results show that TE to $He(1s2p^1P)$ is dominant in the entire energy region we considered. Furthermore, the cross sections for both TE to $He(1s2s^1S)$ and TE to $He(1s2p^1P)$ show similar structures with a clear valley centered at about 25 keV/u and extending from 8 keV/u to 70 keV/u. Similarly, for TE to $He(1s3s^1S)$, the cross sections exhibit impact-energy-dependent oscillatory structures with two valleys located at 1–8 and 8 keV/u–70 keV/u, respectively. Before commenting on this complex behavior, we compare our results with the existing data. As can be observed in Fig. 1, our results show the best overall agreement with available experimental results.[9,12,16,19] It is only for TE to $He(1s3s^1S)$ at $E < 3$ keV/u that our results lie above the experimental data of Ref. 9, with a different slope. This disagreement might be due to the lack of higher excited states correlating with He(1*s*3*d*) in the present GTO basis sets. Since only one series of measurements exists in this energy region, and the values of the cross sections are quite small ($<5 \times 10^{-18}$ cm^2), we cannot draw conclusions from that deviation or confirm the structure of the first valley around 1 keV/u–8 keV/u.

From a comparison with the theoretical calculations, it can be seen that the results of Sural *et al.*[20] are about two times larger than our results as well as the experimental data.[16] The calculations by Hildenbrand *et al.*[7] show better agreement with our results, except that their results lie sometimes lower or higher at different overlapping impact energies. The discrepancies between our results and the other two calculations may be due to the fact that only 6 and 128 channels, respectively, were used in these treatments, whereas we included 1260 channels in our calculations, for which the convergence has also been checked, as already mentioned.

To gain insight into the valley structure exhibited by the cross sections for TE to singlet He excited states at about 25 keV/u, we present in Fig. 2 the cross sections for two resonant processes, namely, TE and electron transfer (ET) to a singlet He excited state,

$$\begin{aligned} &He^+(1s) + He(1s^2) \rightarrow He^+(1s) + He^*(1snl^1L)\ \text{(TE)},\\ &He^+(1s) + He(1s^2) \rightarrow He^*(1snl^1L) + He^+(1s)\ \text{(ET)}, \end{aligned} \tag{10}$$

with $nl = 2s, 2p$, and 3*s*. Note that the validity of our calculations for ET processes is supported by the comparison with experimental data, as shown in our previous work (see Fig. 9 in Ref. 4). It can be observed that the magnitudes of the cross sections for populating $He(1s2s^1S$, $1s2p^1P$, and $1s3s^1S)$, respectively, by either excitation or capture processes are comparable for $E < 8$ keV/u but that their convergence due to symmetry is not reached at our lowest considered energy. However, each of the ET cross sections exhibits a maximum at an energy in the range from around 8 keV/u to 70 keV/u, followed by a rapid decrease for increasing energies. These maxima are located in the same energy region as the valley structure observed in the cross

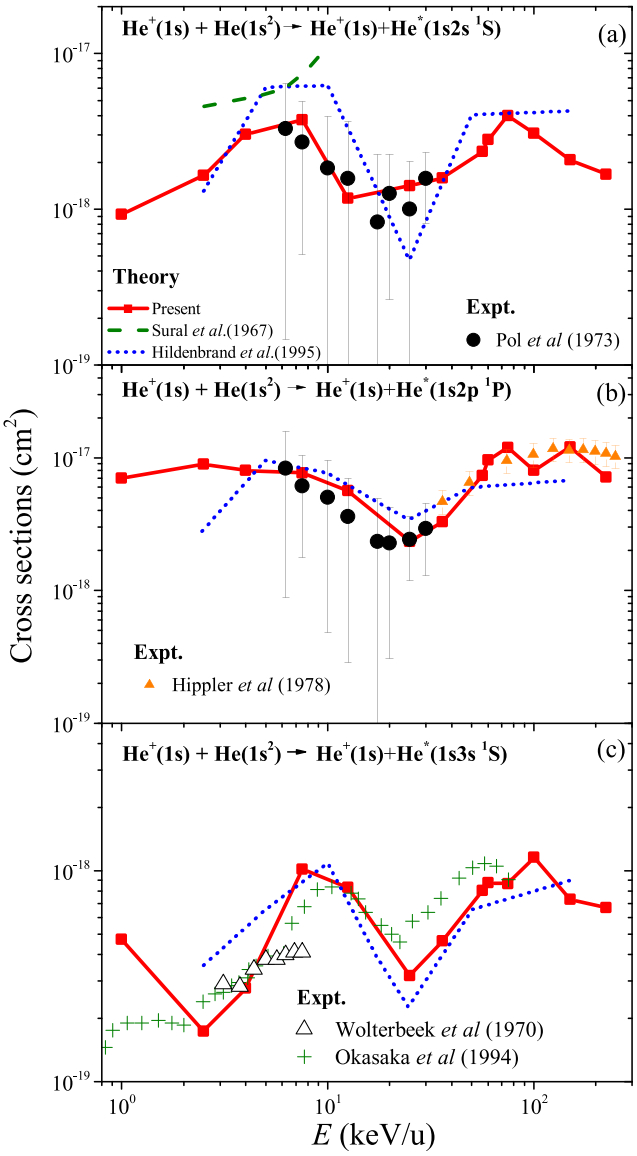

FIG. 1. Cross sections as functions of impact energy for TE to $He(1s2s^1S$, $1s2p^1P$, and $1s3s^1S)$ excited states.

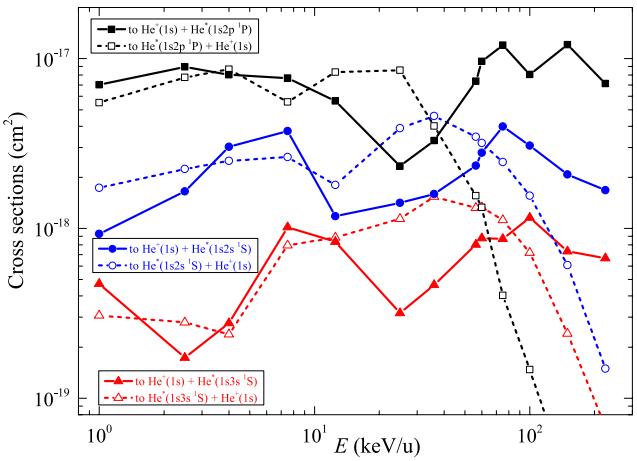

FIG. 2. Cross sections as functions of impact energy for TE and ET to He(1s2s ^{1}S, 1s2p ^{1}P, and 1s3s ^{1}S) excited states. Note that the ET cross sections were presented in Ref. 4.

sections for TE to singlet He excited states, indicating the existence of strong competition between TE and ET resonant processes.

In Figs. 3(a)–3(c), the cross sections for TE to triplet He($1s2s^3S$, $1s2p^3P$, and $1s3s^3S$) excited states, respectively, are presented, together with theoretical[7,20] and experimental[9,16] results for comparison. Note that since the Hamiltonian does not contain spin-dependent interactions, triplet states can only be excited by an exchange of electrons between target and projectile. From a comparison with the results for TE to singlet He excited states shown in Figs. 1(a)–1(c), it is found that (i) the cross sections for TE to triplet He excited states have about the same values at low energy and are sometimes higher than those for TE to singlet He excited states, although TE to triplet states requires an exchange of electrons with the projectile; (ii) a rapid decrease appears at lower energies for TE to He($1s2s$ and $1s3s^1S$) excited states; (iii) there are no valley structures in the cross sections for TE to triplet He excited states. We mention here that we have investigated ET processes to triplet states in Ref. 4. Although the corresponding cross sections are of the same order of magnitude as those for TE processes, no competition between ET and TE is observed in the case of triplet states. A possible reason for the contrast between the singlet and triplet cases may come from the different mechanisms for TE and ET to singlet and to triplet states. In the triplet case, TE can only take place by an exchange of electrons between target and projectile, as indicated above. ET to triplet states is, however, possible through direct electron transfer. In the singlet case, both TE and ET can be achieved by direct electron transition.

For TE to triplet He($1s2s^3S$ and $1s2p^3P$), our results are in very good agreement with experimental results[16] in the overlapping energy region. Note that it was indicated in Ref. 16 that the experimental data for the two lowest-energy points may be too low owing to scattering outside the angular range of the detector, which might explain the small disagreement with our results. The theoretical calculations of Hildenbrand *et al.*[7] overestimate the experimental data[16] by a factor of two, which again may be due to the limited number of channels included in their calculations. For TE to the higher triplet He($1s3s^3S$) excited state shown in Fig. 3(c), our results are in less satisfactory agreement with the only available series of data.[9] Similarly to the TE process to He($1s3s^1S$) at $E < 3$ keV/u, the disagreement is probably due to the lack of higher excited states in the present calculations. Further theoretical and experimental investigations are needed to allow definite conclusions to be drawn.

We next investigate the excitation of the projectile ion He^+. In comparison with TE processes, investigations of projectile excitation (PE) have been much scarcer. In Fig. 4, we present the cross sections for PE to the $He^+(n = 2)$ level in order to provide a comparison with the only existing experimental[16] and theoretical[7] results. To the best of our knowledge, no theoretical or experimental investigations are

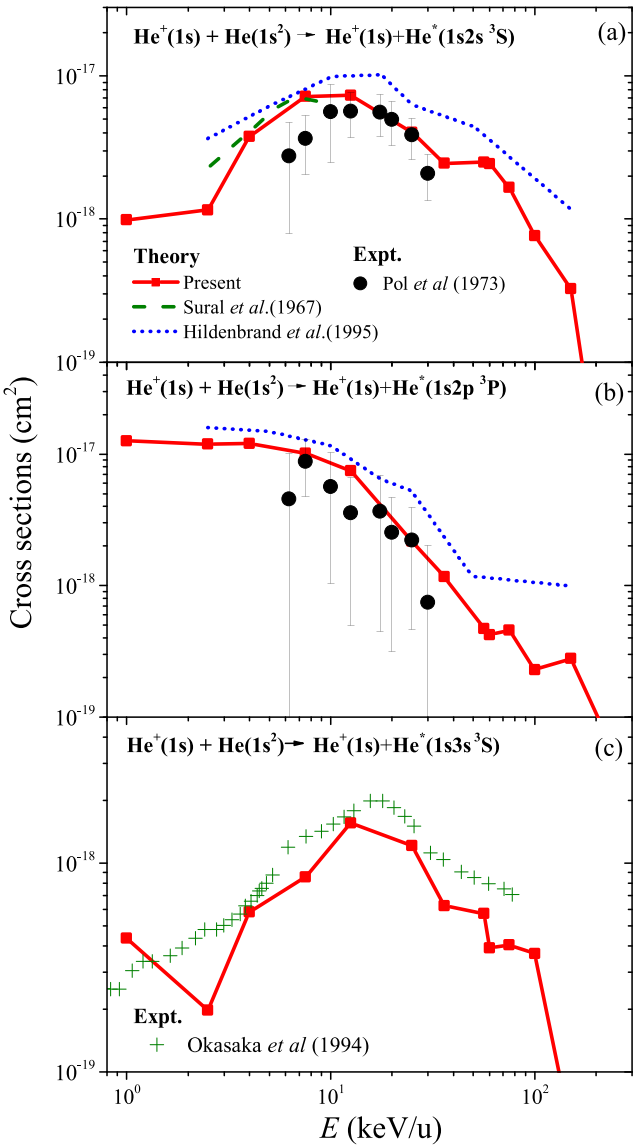

FIG. 3. Cross sections as functions of impact energy for TE to He($1s2s^3S$, $1s2p^3P$, and $1s3s^3S$) excited states.

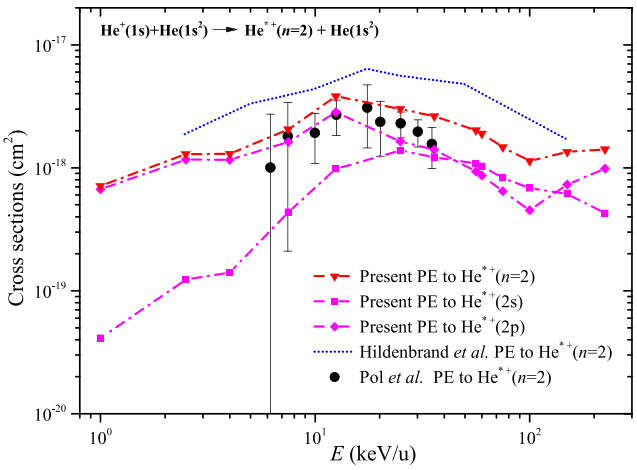

FIG. 4. Cross sections as functions of impact energy for PE to He$*^+(n = 2)$ states. Note that the data for PE to the He$*^+(2p)$ state was presented in previous work.[4]

available for other PE processes. As can be seen from Fig. 4, the cross sections for PE to $He^+(n = 2)$ increase steadily to a maximum located at about 12 keV/u. The cross sections decrease at higher energies and exhibit a shallow valley around 100 keV/u. From a comparison with the existing data, it can be seen that our results are in good agreement with the experimental results of Pol *et al.*,[16] while the calculations by Hildenbrand *et al.*[7] again overestimate the experimental data[16] by a factor of two. It can also be observed that the cross sections for PE to $He^+(2p)$ excited states are dominant for impact energies lower than 50 keV/u. For $E > 50$ keV/u, the cross sections for PE to $He^+(2s)$ excited states become comparable to those for PE to $He^+(2p)$ excited states. Furthermore, the cross sections for PE to $He^+(2p)$ excited states exhibit an oscillatory energy dependence, which has been attributed to strong competition with a two-electron process, namely, ET and TE.[4]

IV. CONCLUSIONS

In this paper, the processes of projectile and target excitation (PE and TE) occurring in the course of He^+ + He collisions have been theoretically investigated. We have used a three-electron semiclassical asymptotic-state close-coupling approach. Furthermore, we have studied a wide collision energy region ranging from 1 keV/u to 225 keV/u, which extends previous predictions to high energies. Overall, our present calculations agree well with available measurements for both PE and TE in the respective overlapping energy regions. However, for TE to He($1s3s\,^3S$) [and also TE to He($1s3s\,^1S$) at $E < 3$ keV/u], our results are in less satisfactory agreement with the only available series of data,[9] which may be due to the lack of well-described high excited states in the basis set used in the present calculations. Further theoretical and experimental investigations would be useful to allow definite conclusions to be drawn.

A comparison of our results with those of other theoretical calculations further demonstrates the importance of nonperturbative calculations in which a sufficient number of channels are taken into account. Furthermore, the cross sections for all the considered TE to singlet He excited states show a valley structure located at about 25 keV/u. We attribute this to competition between the TE and ET to the resonant singlet excited states centered on the projectile. The oscillatory energy dependence of the cross sections for PE to $He^+(2p)$ excited states is due to competition with a two-electron process, namely ET and TE.[4] Our work brings insights into electronic excitation processes and provides new data that are beneficial for many applications, such as modeling of astrophysical[23–25] and laboratory[26–28] plasmas.

ACKNOWLEDGMENTS

This work is supported by the National Natural Science Foundation of China (Grant Nos. 11934004 and 11704040), the National Key Research and Development Program of China (Grant No. 2017YFA0402300) and the CAEP Foundation (Grant No. YZJJLX2017010). Z.H. is supported by the CAEP Foundation (Grant No. CX2019022) and the National Nature Science Foundation of China (Grant No. 11675158). This project has received funding from the LABEX Plas@par (Grant No. ANR-11-IDEX-0004-02).

REFERENCES

[1]D. L. Guo, X. Ma, R. T. Zhang, S. F. Zhang, X. L. Zhu, W. T. Feng, Y. Gao, B. Hai, M. Zhang, H. B. Wang, and Z. K. Huang, "State-selective electron capture in 30- and 100-keV He^++He collisions," Phys. Rev. A **95**, 012707 (2017).
[2]M. S. Schöffler, J. Titze, L. P. H. Schmidt, T. Jahnke, N. Neumann, O. Jagutzki, H. Schmidt-Böcking, R. Dörner, and I. Mančev, "State-selective differential cross sections for single and double electron capture in $He^{+,2+}$-He and *p*-He collisions," Phys. Rev. A **79**, 064701 (2009).
[3]M. Baxter, T. Kirchner, and E. Engel, "Time-dependent spin-density-functional-theory description of He^+-He collisions," Phys. Rev. A **96**, 032708 (2017).
[4]J. W. Gao, Y. Wu, J. G. Wang, N. Sisourat, and A. Dubois, "State-selective electron transfer in He^+ + He collisions at intermediate energies," Phys. Rev. A **97**, 052709 (2018).
[5]I. Mančev, "Four-body continuum-distorted-wave model for charge exchange between hydrogenlike projectiles and atoms," Phys. Rev. A **75**, 052716 (2007).
[6]H. Atan, W. Steckelmacher, and M. W. Lucas, "Single electron loss and single electron capture for 0.6-2.2 MeV He^+ colliding with rare gases," J. Phys. B: At., Mol. Opt. Phys. **24**, 2559–2569 (1999).
[7]R. Hildenbrand, N. Grun, and W. Scheid, "Coupled channel calculations with Cartesian Gaussian basis functions for H + He and He^+ + He reactions," J. Phys. B: At., Mol. Opt. Phys. **28**, 4781–4798 (1999).
[8]J. L. Forest, J. A. Tanis, S. M. Ferguson, R. R. Haar, K. Lifrieri, and V. L. Plano, "Single and double ionization of helium by intermediate-to-high-velocity He^+ projectiles," Phys. Rev. A **52**, 350–356 (1995).
[9]R. Okasaka, K. Kawabe, S. Kawamoto, M. Tani, H. Kuma, T. Iwai, K. Mita, and A. Iwamae, "Excitation functions of He(n=3) levels in the intermediate-velocity regime of He^+-He collisions," Phys. Rev. A **49**, 246–254 (1994).
[10]R. D. DuBois and S. T. Manson, "Electron emission in He^+-atom and He^+-molecule collisions: A combined experimental and theoretical study," Phys. Rev. A **42**, 1222–1230 (1990).
[11]N. V. de Castro Faria, F. L. Freire, and A. G. de Pinho, "Electron loss and capture by fast helium ions in noble gases," Phys. Rev. A **37**, 280–283 (1988).
[12]R. Hippler, K.-H. Schartner, and H. F. Beyer, "Direct and charge-exchange excitation of the 2^1P level in He^+-He collisions," J. Phys. B: At., Mol. Opt. Phys. **11**, L337–L341 (1978).
[13]R. Hegerberg, T. Stefansson, and M. T. Elford, "Measurement of the symmetric charge-exchange cross section in helium and argon in the impact energy range 1-10 keV," J. Phys. B: At., Mol. Opt. Phys. **11**, 133–147 (1978).
[14]E. A. Hinds and R. Novick, "Precise resonant charge-transfer cross sections for He-He^+ between 2 eV and 100 eV," J. Phys. B: At., Mol. Opt. Phys. **11**, 2201–2207 (1978).
[15]T. G. Winter and C. C. Lin, "Electron capture into excited states of helium by helium-ion impact on helium," Phys. Rev. A **12**, 434–443 (1975).

[16]V. Pol, W. Kauppila, and J. T. Park, "Absolute differential elastic- and inelastic-scattering cross sections in 25-140 keV He^+ + He collisions," Phys. Rev. A **8**, 2990–3000 (1973).
[17]M. Barat, D. Dhuicq, R. Francois, R. McCarroll, R. D. Piacentini, and A. Salin, "Inelastic processes in He^+-He collisions," J. Phys. B: At., Mol. Opt. Phys. **5**, 1343–1350 (1972).
[18]W. N. Shelton and P. A. Stoycheff, "Measurement of the total cross section for single-electron transfer in collisions of He^+ with He in the energy range 2-22 keV," Phys. Rev. A **3**, 613–619 (1971).
[19]L. Wolterbeek Muller and F. J. De Heer, "Electron capture into excited states by helium ions incident of noble gases," Physica **48**, 345–396 (1970).
[20]D. P. Sural, S. C. Mukherjee, and N. C. Sil, "Electron capture and excitation in He^+-He collisions," Phys. Rev. **164**, 156–165 (1967).
[21]C. F. Barnett and P. M. Stier, "Charge exchange cross sections for helium ions in gases," Phys. Rev. **109**, 385–390 (1958).
[22]W. Lichten, "Resonant charge exchange in atomic collisions," Phys. Rev. **131**, 229–238 (1963).
[23]E. Möbius, D. Hovestadt, B. Klecker, M. Scholer, G. Gloeckler, and F. M. Ipavich, "Direct observation of He^+ pick-up ions of interstellar origin in the solar wind," Nature **318**, 426–429 (1985).
[24]C. J. Joyce, C. W. Smith, P. A. Isenberg, N. Murphy, and N. A. Schwadron, "Excitation of low-frequency waves in the solar wind by newborn intersteller pickup ions H^+ and He^+ as seen by voyager at 4.5 AU," Astrophys. J. **724**, 1256–1261 (2010).
[25]P. Swaczyna, D. J. McComas, and E. J. Zirnstein, "He^+ ions comoving with the solar wind in the outer heliosphere," Astrophys. J. **875**, 36 (2019).
[26]R. K. Janev, "Atomic collisions in fusion plasma," J. Phys. Colloq. **50**, C1-421–C1-443 (1989).
[27]A. A. Korotkov and R. K. Janev, "Attenuation of energetic helium beams in fusion plasmas," Phys. Plasmas **3**, 1512–1523 (1996).
[28]*Atomic and Plasma–Material Interaction Data for Fusion*, edited by R. E. H. Clark (International Atomic Energy Agency, Vienna, Austria, 2001).
[29]N. Sisourat, I. Pilskog, and A. Dubois, "Nonperturbative treatment of multi-electron processes in ion-molecule scattering: Application to He^{2+}-H_2 collisions," Phys. Rev. A **84**, 052722 (2011).
[30]J. W. Gao, Y. Wu, N. Sisourat, J. G. Wang, and A. Dubois, "Single- and double-electron transfer in low- and intermediate-energy C^{4+} + He collisions," Phys. Rev. A **96**, 052703 (2017).
[31]J. W. Gao, Y. Wu, J. G. Wang, A. Dubois, and N. Sisourat, "Double electron capture in H^+ + H^- collisions," Phys. Rev. Lett. **122**, 093402 (2019).
[32]L. Shampine and M. Gordon, *Computer Solution of Ordinary Differential Equations: The Initial Value Problem* (Freeman, San Francisco, CA, 1975).
[33]A. Kramida, Yu. Ralchenko, J. Reader, and NIST ASD Team, *NIST Atomic Spectra Database* (ver. 5.7.1), available at: https://physics.nist.gov/asd, October 15, 2020, National Institute of Standards and Technology, Gaithersburg, MD, 2019.